


**ORIGINAL ARTICLE** OPEN ACCESS

# Multispectral Imaging Flow Cytometry for Spatio-Temporal Pollen Trait Variation Measurements of Insect-Pollinated Plants

Franziska Walther<sup>1,2</sup> | Martin Hofmann<sup>3</sup> | Demetra Rakosy<sup>2,4,5</sup> | Carolin Plos<sup>2,6</sup> | Till J. Deilmann<sup>7,8</sup> | Annalena Lenk<sup>7,9</sup> | Christine Römermann<sup>2,7,8</sup> | W. Stanley Harpole<sup>1,2,6</sup> | Thomas Hornick<sup>1,2</sup> | Susanne Dunker<sup>1,2</sup>

<sup>1</sup>Department Physiological Diversity, Helmholtz Centre for Environmental Research UFZ, Leipzig, Germany | <sup>2</sup>German Centre for Integrative Biodiversity Research iDiv Halle-Jena-Leipzig, Leipzig, Germany | <sup>3</sup>Technische Universität Ilmenau, Ilmenau, Germany | <sup>4</sup>Department Community Ecology, Helmholtz Centre for Environmental Research UFZ, Leipzig, Germany | <sup>5</sup>Thuenen Institute of Biodiversity, Braunschweig, Germany | <sup>6</sup>Martin-Luther-Universität Halle-Wittenberg, Halle, Germany | <sup>7</sup>Institute of Ecology and Evolution, Friedrich-Schiller-Universität Jena, Jena, Germany | <sup>8</sup>Senckenberg Institute for Plant Form and Function, Jena, Germany | <sup>9</sup>Universität Leipzig, Leipzig, Germany

**Correspondence:** Susanne Dunker ([susanne.dunker@ufz.de](mailto:susanne.dunker@ufz.de))

**Received:** 3 June 2024 | **Revised:** 18 March 2025 | **Accepted:** 26 March 2025

**Funding:** This work was supported by Bundesministerium für Ernährung und Landwirtschaft, 2819NA102, 2819NA106. Deutsche Forschungsgemeinschaft, 09159715, 09159723, 34600830-13, 346001057-01. DEAL.

**Keywords:** interspecific variation | intraspecific variation | machine learning | multispectral image-based flow cytometer | pollen analysis | reference database | spatial and temporal variation

## ABSTRACT

Artificial intelligence (AI) surpasses human accuracy in identifying ordinary objects, but it is still challenging for AI to be competitive in pollen grain identification. One reason for this gap is the extensive trait variation in pollen grains. In classical textbooks, pollen size relies on only 25–50 pollen grains, mostly for one plant and site. Lack of variation in pollen databases can cause limited application of machine learning approaches to real-world samples. Therefore, our study aims to investigate sources of spatial and temporal pollen trait variation for pollen morphology and fluorescence. For this purpose, 64,001 pollen grains from the four herbaceous and insect-pollinated plant species *Achillea millefolium* L., *Lamium album* L., *Lathyrus vernus* (L.) Bernh., and *Lotus corniculatus* L. sampled across four years and seven locations across Central Germany were measured using multispectral imaging flow cytometry. Observed trait variations were very species-specific; however, for most species, significant differences in spatial as well as temporal variation were found for at least one pollen trait. We could also show that this variability and the identity of a particular sample influence the accuracy of AI classifications and that multiple measurements of different origins provide the most robust AI-based identifications.

## 1 | Introduction

Pollen grains are the haploid microspores of seed plants and an essential part of their reproduction [1]. In 78% of temperate

zone plants, reproduction depends on the transfer of pollen by animals—in most cases by insects [2–7]. Pollen transfer patterns offer insights into plant–pollinator interaction networks and the quality and quantity of the pollination services

Thomas Hornick and Susanne Dunker are shared senior authors.

This is an open access article under the terms of the [Creative Commons Attribution](https://creativecommons.org/licenses/by/4.0/) License, which permits use, distribution and reproduction in any medium, provided the original work is properly cited.

© 2025 The Author(s). *Cytometry Part A* published by Wiley Periodicals LLC on behalf of International Society for Advancement of Cytometry.

provided [8–13]. For the ease of use, plant–pollinator interaction networks are often constructed based on the monitoring of flower-visiting insects to understand the dependencies of plants and pollinators [14]. But plant visitor-based networks have limited explanatory power in terms of pollen transfer, which is why it is important to also have methods at hand to determine pollen identity and quantity directly from the pollinators via microscopic methods [14]. Changes in the structure of these networks under diverse anthropogenic pressures may lead to high economic losses, a further decline in plant and animal diversity, reduced food production security, and the collapse of entire ecosystems [7, 15, 16].

### 1.1 | Traditional Pollen Identification

Accurate species identification and quantification are important in the context of plant–pollinator interactions and even beyond, including applications in ecology, agriculture, and air quality monitoring [17–20]. Pollen can be assigned to the respective plant species based on their size and diverse morphological features [21–24]. The traditional method for pollen analysis via manual microscopy (i.e., “gold standard”) is, however, expert-requiring and time-intensive and does not always allow the accurate identification of pollen grains below the genus or even family level. For these analyses, usually, size, shape, and sculpture type are used as distinguishing features [21, 22]. These diagnostic features are, however, often based on a maximum of 50 grains of one plant individual collected at one site (e.g., [21, 25–27]). As a consequence, little of the natural spatial and temporal variation of pollen traits is taken into account. A similar situation can be observed in the main pollen databases for Central Europe (e.g., Pollen-Wiki (<https://pollen.tstebler.ch/>); PalDat (<https://www.paldat.org/>)).

### 1.2 | Automated Pollen Identification

Nowadays, the trend is towards more automated pollen identification, as it has the potential to be more cost-effective, time-efficient, and reproducible. Such automated methods for pollen image acquisition are based, for example, on automated slide scanning microscopy [20] or multispectral imaging flow cytometry (MIFC) [28, 29]. Creation of pollen recognition models requires a training data set of labeled (ground truth) images, which were curated by a taxonomic expert. Based on these images, the model can identify features, which enable the best discrimination of the image classes defined by the expert. Image-based classification approaches rely on a large quantity of labeled (ground-truth) images [20, 30–35] and depending on the type of images require a minimum of 75–100 images per class [28, 36, 37]. Although several AI-based classifiers show high performance on benchmark datasets, they fail to transfer the same degree of accuracy to more challenging testing conditions, such as real-world scenarios [38]. This is likely due to the fact that the training input data should ideally encompass as much variation as possible, ensuring that it is as close as possible to what is expected in the data to be predicted [39]. To achieve this, we require a better understanding of the extent of total pollen trait variation in response to spatio-temporal changes in the environment.

### 1.3 | Inter- and Intra-Specific Pollen Trait Variation

Interspecific variation in pollen traits, especially in pollen size, shape, and surface structure, is high [40]. From an ecological and evolutionary point of view, one would assume a high conservatism of intraspecific pollen size, as sexual reproduction can only be successful if the size and position of reproductive organs within the flower fit together [41], for example, there are constraints related to pollen volume and pistil length [42]. A small difference therein can result in changes in pollen flow and, by that, pollination efficiency [43]. Several studies suggest that species differ in non-pollen floral traits in response to environmental variation (e.g., [44, 45]) and some studies have shown that intraspecific variation of pollen traits can arise from differences in ploidy [46–52], nutritional supply [53–55] as well as temporal and spatial patterns [56–58]. Evolutionarily, pollen shape and size may be influenced by ecological factors such as shifts in the mode of pollination or changes in pollen volume to adapt to water availability [59].

It has been shown that ploidy level differences can be distinguished using pollen volume measurements [52]. In addition to ploidy as a source of pollen volume variation, Bell [53] could show that mineral nutrition affects pollen size for agriculturally relevant species such as tomato (*Solanum lycopersicum* (L.)), corn (*Zea mays* (L.)) and dill (*Anethum graveolens* (L.)). For *Corylus avellana* (L.) Frenguelli et al. [57] could show that within a flowering season, the size and shape of pollen vary, resulting in a proportional change from undeveloped, developed, and dehydrated pollen. Kremer et al. [58] studied temporal and spatial sources of pollen size variation in *Fraxinus pennsylvanica* (Marshall) and *Fraxinus americana* (L.) collected during two years in Croatia and Canada. The authors found that the pollen size of both species was so variable that it could not be used as a differentiating feature for the two species, although the mean size difference should be large enough to allow microscopic differentiation [58]. A similar pattern was revealed for *Betula* species by Mäkelä [60].

Most studies on intraspecific trait variation have focused on pollen size and/or pollen shape of wind-pollinated or agriculturally relevant insect-pollinated species, and not on grassland insect-pollinated plant species or “new traits” such as pollen fluorescence, a potential indicator of pollinator visual attractants [28]. When using MIFC for pollen analysis, several fluorescence images for different spectral ranges of the investigated particles can be derived in addition to brightfield images [28]. Pollen autofluorescence and its associated variation are understudied phenomena. Based on a limited number of studies on pollen fluorescence [61, 62] intraspecific variation can be assumed to be high as well for this trait, since the chemical composition of fluorescing molecules might be strongly influenced by environmental conditions. As the main function of pollen is the transfer of DNA, and especially at sun-exposed sites, a higher content of photo-protective carotenoids protecting the DNA from damage might result in a higher pollen pigment concentration and thereby changes in fluorescence patterns. In addition to (spatio-temporal) variations in the environment, we can assume temporal variations in pollen fluorescence across the season: the phenological development of pollen is expected to be related to

changes in pollen fluorescence as the pollen exine is formed by an oxidative polymerization of carotenoid compounds [63].

This exploratory study aims to assess the most important potential sources of pollen trait variation of four common Central European insect-pollinated herbaceous grassland plant species, which were sampled across distinct sites and years varying in environmental conditions. We thereby explored the intraspecific and interspecific spatial and temporal variation of “traditional” morphological pollen traits (e.g., size, shape), but also for the first time pollen fluorescence, traits derived from multispectral imaging flow cytometry (MIFC). In line with our objectives, we base our approach on the following expectations:

1. We expect significant inter- and intra-specific variation in traditional morphological traits (e.g., pollen size and shape) and fluorescence traits of fully developed pollen across diverse habitats and years. This variation is relevant both for ecological insights and for advancing pollen classification using image-based analysis.
2. We expect intra-annual variation in pollen size, shape, and fluorescence to correspond with different phenological stages of the pollen (undeveloped—developed), providing valuable insights into ecological dynamics and enhancing the precision of automated classification methods.

Additionally, we conducted a machine-learning experiment to analyze the variation of the collected pollen species images depending on the sampling location and time in order to determine how the variation captured in the images changes the ability of the classifier to predict the correct species. More precisely, we examined the following questions:

3. How does trait variation influence classification accuracy?
4. Is one pollen measurement, consisting of about 600 pollen grains, sufficient to classify species correctly?

## 2 | Methods

### 2.1 | Sampling

For this study, pollen samples of the following four common European insect-pollinated herbaceous plant species were used: *Achillea millefolium* L. (Asteraceae), *Lamium album* L. (Lamiaceae), *Lathyrus vernus* (L.) Bernh. (Fabaceae) and *Lotus corniculatus* L. (Fabaceae), all with a similar distribution range (Table S1). Sampling took place from 2019 to 2022 in the framework of two different projects (PhenObs and NutriBee). PhenObs is a global network of botanical gardens studying climate change related phenology patterns of herbaceous plants and the NutriBee project aimed to create a national pollen library for automated recognition and quantification of insect-relevant pollen. The samples from the four common species provide an overview of the possible extent of pollen trait variation. Despite the heterogeneous nature of the data, the present dataset provides a unique opportunity to estimate the extent of pollen size and morphological variation. Anthers of the four species were collected from seven different sites across four German cities: Berlin (B), Halle (H), Jena (J), as part of the PhenObs network

[64], and Leipzig (L) as part of the NutriBee project, (Figure S1 and Table S2). The collection sites included semi-natural dry grasslands (SDG), mesophilic grasslands (MPG) in Jena (see [44] for a description of these sites), botanical gardens (BG), and an urban open space site in Leipzig's northern district, Eutritzsch (referred to as 'NO'). In Berlin and Halle, pollen samples were collected exclusively from the botanical gardens. In Jena, pollen samples were collected from the botanical garden as well as from SDG and MPG sites, which differ primarily in soil moisture, soil nutrients, inclination, and aspect, leading to variations in light intensity.

For *L. album* and *L. vernus*, three to seven samples were additionally collected at three different time points in BG-J within 1 year to investigate the impact of phenology on pollen traits. The respective time points of sampling included “First Flowering Day” (FFD), the “Peak Flowering Day” (PFD; first day of peak (maximum) flowering) and the “Last Flowering Day” (LFD; last day of flowering) according to the sampling protocol of the PhenObs project. For the phenological analysis of pollen trait variation all pollen were considered, while for the other cases pollen traits were only derived from fully developed/ripe pollen.

An overview of the examined pollen samples, including the location, time of collection, and quantity, can be found in the supplement (Table 1, Table S2). Anthers were either transferred directly into a 2 mL Eppendorf tube with clean forceps, or the whole flower was collected in paper bags, and the respective anthers were later transferred to a 2 mL Eppendorf tube in the laboratory. All samples were stored at  $-20^{\circ}\text{C}$  until further analysis. For *A. millefolium*, multiple flower heads of 2–3 individuals were collected for each sample. For *L. album*, the anthers of 2–5 flowers from seven individuals were collected for each sample. For *L. vernus* and *L. corniculatus*, anthers of 1–10 flowers from seven individuals were collected for each sample.

### 2.2 | Sample Preparation

All samples were prepared according to Dunker et al. [28] with an additional washing step with 500  $\mu\text{L}$  D-PBS (Dulbecco's phosphate buffered saline (without calcium and magnesium), Biowest, Nuaille, France), centrifuging and removing the supernatant. In brief, fully matured anthers or, for small flowers, whole inflorescences were collected from individual plants and placed in 2 mL Eppendorf tubes with pollen isolation buffer. Release of pollen was induced by vortexing and a 5 min sonication step, followed by a filtration step with a 50  $\mu\text{m}$  filter (CellTrics, Sysmex, Norderstedt, Germany). Filtering removed plant/flower fragments while retaining pollen. Subsequently, the samples were centrifuged, the supernatant was discarded, and D-PBS was added.

### 2.3 | Multispectral Imaging Flow Cytometry (MIFC)

Samples were measured with an Imagestream X Mk II imaging flow cytometer (Amnis part of Cytek, Amsterdam, Netherlands) connected to an autosampler at 40 $\times$  magnification according to Dunker et al. [28] with one laser (488 nm laser with 5 mW

**TABLE 1** | Overview of (a) number of analyzed developed pollen per site and (b) trait ranges (rounded min.—max.) of the assessed six pollen traits by MIFC as well as the given size range from literature described in [21] for each species (BG—botanical garden, MPG—mesophilic grasslands, NO—urban open space, SDG—semi-natural dry grasslands).

Section	City	Site	Year	<i>Achillea millefolium</i>	<i>Lamium album</i>	<i>Lathyrus vernus</i>	<i>Lotus corniculatus</i>	Total
(a)	Berlin	BG	2020	—	598	—	—	598
	Halle	BG	2019	—	457	5,083	—	5,540
	Halle	BG	2020	—	210	—	—	210
	Leipzig	BG	2019	—	—	2,448	5,249	7,697
	Leipzig	BG	2022	—	—	—	—	—
	Jena	BG	2019	—	—	8,721	—	8,721
	Jena	BG	2020	431	86	666	—	1,183
	Jena	BG	2021	6,497	—	—	—	6,497
	Jena	SDG	2020	234	—	—	4,948	5,182
	Jena	MPG	2020	1,111	—	—	4,024	5,135
	Leipzig	NO	2022	—	—	—	23,238	23,238
			Total	8,273	1,351	16,918	37,459	64,001
			Average	212	79	1,128	1,249	
(b)			Circularity	15.5–22.3	14.1–24.4	11.4–24.4	12.4–23.8	
			Circularity	15.5–22.3	14.1–24.4	11.4–24.4	12.4–23.8	
			Compactness	0.7–0.8	0.5–0.7	0.5–0.6	0.6–0.7	
			Elongatedness	1.0–1.1	1.0–1.2	1.0–1.2	1.1–1.2	
			Intensity Ch02	297,421–624,259	108,079–279,165	110,403–345,844	12,753–279,148	
			Intensity Ch05	266,305–1,366,096	48,761–519,005	61,824–191,904	3,839–66,833	
			Size (µm)	28.0–32.0	26.0–28.5	32.0–35.5	15.0–20.0	
		Reference Size (µm) [21]	27.5–35.8	22.5–30.3	35.8–40.5	15.9–21.2		

Note: Only developed pollen was considered in the analysis.

intensity). The instrument is a special-order instrument with non-co-linear laser configuration (patent submission Dunker 2019 EP000003692357A1/US020200278300A1). For each individual pollen grain passing the light sources, separate microscopic images were captured by two independent CCD cameras of the ImageStream X Mk II, resulting in brightfield, fluorescence, and scatter images. In our study, for all pollen samples, only autofluorescence was measured; no fluorescence staining was applied. The measurement was stopped when either 5000 particles were measured or after 10 min when less than 5000 particles were possible to collect.

## 2.4 | Image Extraction and Annotation

In-focus images of single pollen grains that allowed for the correct estimation of pollen traits of whole pollen grains were separated from debris according to Hornick et al. [65] by using a bivariate plot of both brightfield channel intensities (brightfield

channels 1 and 9) in the IDEAS Software (Version 6.2, Amnis part of Cytek, Amsterdam, Netherlands). In contrast to debris particles, pollen grains usually have a brightfield intensity between –6,273,326 and –92,036 (a.u.) (Channel 1) and –3,984,408 and –62,636 (a.u.) (Channel 9). Images of single pollen grains were then separated from images containing multiple pollen grains or pollen with additional debris particles by using particle size as an exclusion criterion. All remaining particle images were manually examined in order to guarantee high data quality by estimating pollen traits of only particle images with single, sharp, and centered pollen grains without non-species-specific pollen or debris attached [65].

## 2.5 | Feature Selection and Extraction

The following traits were examined: Circularity, Compactness, Size, Elongatedness, Intensity Ch02 (green fluorescence intensity, Exc. 488 nm/Em. 528/65 nm) and Intensity Ch05 (red

fluorescence intensity, Ch05—Exc. 488 nm/Em. 702/85 nm) (Table S3). These six traits were selected from different contrasting categories (signal strength (i.e., intensity), size and shape) as well as a selection based on low autocorrelation between different traits (see pair plots with Pearson correlation coefficient in Figures S2–5). In the following, whenever the term ‘Size’ is used, it specifically refers to the pollen trait ‘Length’. The “Length” feature was chosen as the most appropriate size trait following Hornick [65] and all feature calculations were based on an “AdaptiveErode mask,” ensuring a proper fit for all pollen grains with a threshold value of 95% [65]. The “AdaptiveErode mask” identifies pixels around the particle, ensuring that they contact the input boundary with at least a specified minimum radius threshold. This mask then erodes 5% of the particle boundary, as detailed in the IDEAS 6.2 User’s Manual.

## 2.6 | Data and Statistical Analysis

Statistical analyses and figure preparation were conducted using the R software R 4.3.3 [66] and the packages “ggplot2” [67], “vegan” [68], “fmsb” [69] and “ggmaps” [70].

To generally test whether morphological and fluorescence traits of fully developed pollen sampled from different locations are variable, we ran a Permutational Multivariate Analysis of Variance (PERMANOVA, 999 permutations) based on a dissimilarity matrix calculated with euclidean distance plus Post hoc tests with the “pairwiseAdonis” package [71] and an ANOVA with Post hoc tests. The formula for the PERMANOVA was structured as follows: `trait_data (species)~site * year`, where `trait_data` represents the measured trait values for each species, and the analysis assesses the interaction effects of site and year on these traits. The formula for the ANOVA was structured as follows: `response_var factor_var`, where `response_var` is the trait data and `factor_var` is the location, site, year, or day. In this formula, the ANOVA analysis assesses whether there are statistically significant differences in the mean of `response_var` across the different levels of `factor_var`. Furthermore, we used a principal component analysis of multivariate trait data as well as spider plots to visualize temporal and spatial variation for each species.

To analyze whether pollen trait variation is related to phenological stages of the flowers from which pollen samples were taken (BG-J dataset), we performed an ANOVA with Post hoc tests for the two species, *Lamium album* and *Lathyrus vernus*. The underlying dataset for the phenological analyses includes both undeveloped and developed pollen grains analyzed in both equatorial and polar views. The pollen grains were collected in 1 year at one location. To analyze the proportions of undeveloped and developed pollen, outliers were first identified and removed. The classification into undeveloped and developed pollen was based on the pollen trait “size,” as several studies have shown that undeveloped/non-viable and developed/viable pollen can be differentiated by their size [72]. Next, to ensure comparability among the phenological stages, we randomly drew an equal sample size for each stage based on the smallest

sample size available. The threshold value that separates the undeveloped from the developed population was then determined using Kernel Density Estimation (KDE). This threshold was defined as the point between the two modes of the distribution where the KDE curve reaches 10% of its maximum height. Local maxima above this 10% threshold were then identified, representing significant peaks in the data distribution, which may correspond to different populations. The boundary between the two populations was calculated as the average (mean) of these identified maxima. This boundary serves as the optimal point for distinguishing between undeveloped and developed pollen. Based on this calculated boundary, the data were divided into two groups: one comprising pollen sizes less than or equal to the boundary, and the other comprising pollen sizes greater than the boundary.

## 2.7 | Machine Learning

### 2.7.1 | Data Preparation

The machine learning experiment evaluates how well a classifier can recognize pollen species, and it can be tested if samples collected at different locations and times improve or worsen prediction accuracy (Table S8). The experiment has two stages:

In stage one, we ran 48 different configurations. Each configuration focuses on classifying one specific species, location, and time combination in contrast to the other species. We prepared a foundation dataset of four combinations of location and time per species and sampled 20 images of each combination for training and testing. This dataset consisted of 320 images for training and testing, that is, a 50/50 split. Each of the 48 different configurations was based on this foundation dataset. For each run, we focused on one species. The images were replaced by 80 images of one location and time so that we could evaluate each combination of location and time for every species. These combinations added up to 12 per species with different training and testing samples of one species but the same images of the other species. These experiments were repeated five times, randomly initializing the network’s weights, and the mean and standard deviations were reported.

In stage two, we ran 16 additional configurations that now consisted of two and three combinations of locations and times depending on the accuracy achieved in stage one. We divided the additional configurations into two cases. In the first case, we wanted to observe how the learning performance changed if the best-performing data combination was mixed with data from a worse-performing combination. Here, we selected the predicted (test) combination with the highest accuracy for each species and selected the training split that led to this result. We then sampled 40 images from the best training combination (Backward 1) and 40 from the second-best combination (Backward 2)—80 samples in total. Afterward, we randomly sampled 80 samples evenly distributed from the best, second, and third-best combinations (Backward 3). Accordingly, we got a total of eight configurations for the first case. We sampled the images in the second

case like those in the first case but used the worst combinations (Forward 1) and the second (Forward 2) and third-worst cases (Forward 3), respectively.

### 2.7.2 | Data Pre-Processing

Data pre-processing was the same in all experiments. We extracted the images from the cytometry measurements using the same protocol used by Dunker et al. [28]. The images are in a 64-bit integer TIFF format, packed, and loaded with ImageZipDataset (<https://github.com/CeadeS/ImageZipDataset>). All images were scaled into 12 bits per channel, that is, 0 and 4096.

### 2.7.3 | Model Training

Data augmentation, that was a result of extensive parameter tuning, was performed the same way in all experiments. We used a training crop size of 176 with a random scale of 0.08 to 1.2 and a random aspect ratio of 0.7 to 1.3, as well as random rotation  $\pm 27^\circ$  and horizontal and vertical flip of the normalized images. Furthermore, we used random erasing [73], a mixup of 0.2 [74] and cutmix [75] of 1.0 to pre-process the data. If we used the brightfield channel only, we repeated this channel along the channel axis three times to enable the use of RandAugment [76].

We trained the model using Adam [77] with a learning rate of 0.025 with a cosine annealing [78] with five warmup epochs for 100 epochs, a batch size of 64, and weight decay of 0.00002.

We used the ResNet18 [79] with an adaptive average pooling [80] as the last pooling operation.

## 3 | Results

A total of 101 samples from seven locations collected in four consecutive years from the two different projects were available for evaluation. This corresponds to a total of 64,001 developed pollen grains and 768,012 pollen images. On average, the pollen count ranged from 79 to 1,249 pollen per measurement (mean = 634). Most pollen images were available for *L. corniculatus*, whereas *L. album* had the least pollen images of all species (Table 1).

### 3.1 | Inter- and Intra-Specific Spatial and Temporal Variation of Fully Developed Pollen

The pollen grains of *A. millefolium*, *L. album*, and *L. vernus* are similar in size ( $\sim 30\mu\text{m}$ ). In contrast, *L. corniculatus* pollen is smaller, averaging around  $20\mu\text{m}$ , but exhibits the greatest size variation ( $15.0\text{--}20.0\mu\text{m}$ ). Following this, *A. millefolium* shows a size range of  $28.0\text{--}32.0\mu\text{m}$ , *L. vernus* ranges from  $32.0$  to  $35.5\mu\text{m}$ , and *L. album* from  $26.0$  to  $28.5\mu\text{m}$  (Table 1).

The PERMANOVA and subsequent post hoc tests of the multidimensional trait data resemblance matrix revealed overall

significant interspecific differences ( $p=0.018$  for the post hoc test of *L. vernus* vs. *L. corniculatus*) and  $p=0.006$  (all remaining post hoc tests)). Almost all pairwise comparisons are significantly different for individual species and sites, but not for years, except for *L. corniculatus* (Tables S4, S5).

*A. millefolium* and *L. corniculatus* form distinct clusters in the PCA in which they separate on the first two axes that explain together 80.7% of variance (Figure 1). By using the third significant PCA axis, the other two species form distinguishable clusters on PC3 and PC2 (Figure S8).

Intraspecific variation in *A. millefolium* is primarily driven by the two fluorescence intensities, in *L. corniculatus* by pollen elongation, in *L. album* and *L. vernus* more by circularity and pollen size, so in principle, species-specific trends of trait variation could be found across the assessed species (Figure 2). As an example, for the temporal variation, *L. album* showed a comparable pollen size in 2019 and 2020 ( $p=0.833$ ), while *L. vernus* pollen size differed significantly between 2019 and 2020 ( $p=0.003$ ). And vice versa, the intensity of red fluorescence was significantly different in both years for *L. album* ( $p=0.001$ ), while it did not differ for *L. vernus* ( $p=0.382$ ).

As an example, for the spatial variation, *A. millefolium* pollen from MPG was significantly smaller (7%) than pollen collected from SDG ( $p=0.001$ ). The size of the *L. corniculatus* pollen, on the other hand, did not differ between the Jena sites ( $p=0.539$ ). The green fluorescence intensity of *L. album* pollen collected in different botanical gardens in the same year was 22% higher in Berlin than those collected in Halle ( $p=0.009$ ) and even 52% higher than those collected in Jena ( $p<0.001$ ). Even within Leipzig, as in *L. corniculatus* (northern part and botanical garden), pollen size differed significantly by 26% ( $p<0.001$ ) (Table S6).

### 3.2 | Phenological Pollen Trait Variation (Undeveloped and Fully Developed Pollen)

Intra-annual variation related to different phenological stages (FFD, PFD and LFD) could be shown for *L. vernus* for five traits (circularity  $p<0.001$ , elongatedness  $p=0.003$ , green fluorescence intensity  $p=0.01$ , red fluorescence intensity  $p=0.008$  and size  $p=0.004$ ), while no significant variation was observed for *L. album* (Figure 3 and Table S6). For example, *L. vernus* pollen sampled at PFD or LFD was 14% or 3% less circular than pollen sampled at FFD.

For the two species *L. album* and *L. vernus*, the density distribution of the pollen traits “size” and “green fluorescence intensity” was examined (Figure 4). The density distribution of the individual samples can be found in the appendix (Figure S9). The analyzed pollen traits showed a bimodal distribution for both traits that relate to pollen development and/or the proportion between non-developed and fully-developed pollen during flower development. Surprisingly, *L. album* pollen was largest at the first flowering day (modal value:  $26.5\mu\text{m}$ ) and became smaller (peak flowering day—modal value:  $26\mu\text{m}$ ) and smaller within the season (last flowering day—modal value:  $25.5\mu\text{m}$ ). While *L. vernus* pollen grains were, as expected, smallest at the

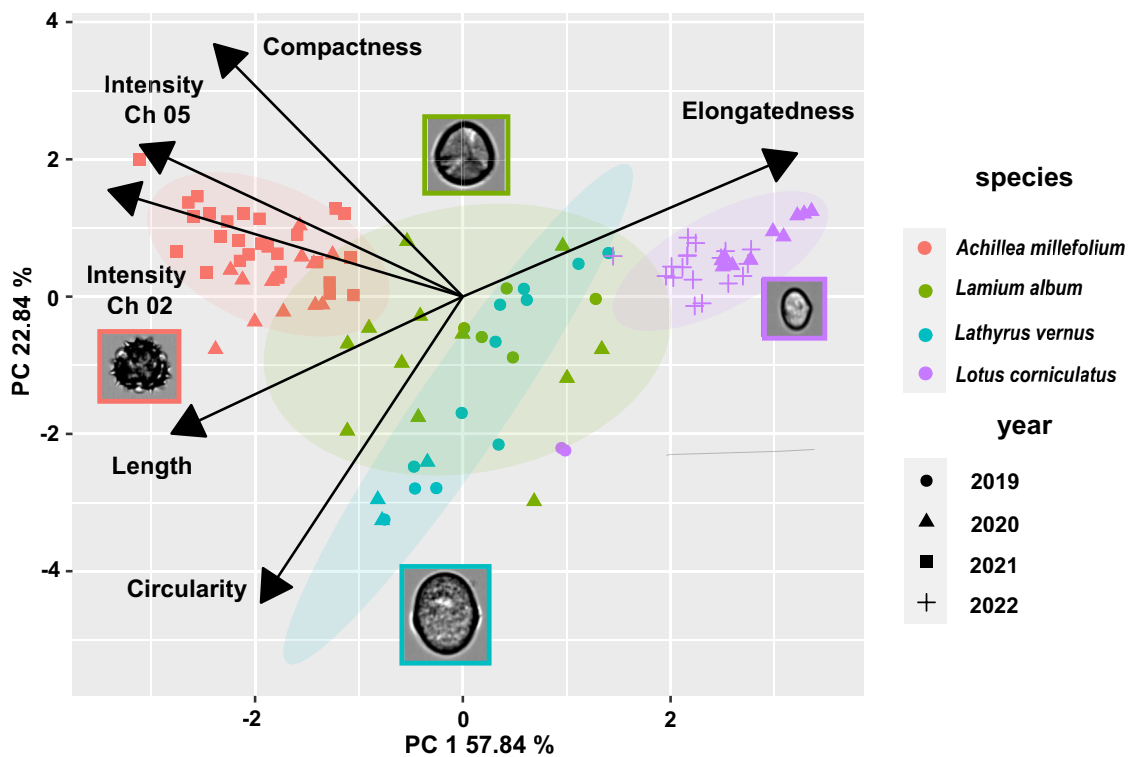


**FIGURE 1** | Principal component analysis of six selected pollen traits circularity, compactness, size, elongatedness, intensity Ch02 (green fluorescence intensity), and intensity Ch05 (red fluorescence intensity) used of the four studied species (*A. millefolium*, *L. album*, *L. vernus*, and *L. corniculatus*) and the year of collection (symbols). The arrows represent the loadings and the images at the corresponding ellipses show a representative microscopic image of the pollen and were taken with MIFC (more detailed PCA in Figures S6–S8). [Color figure can be viewed at [wileyonlinelibrary.com](https://onlinelibrary.wiley.com)]

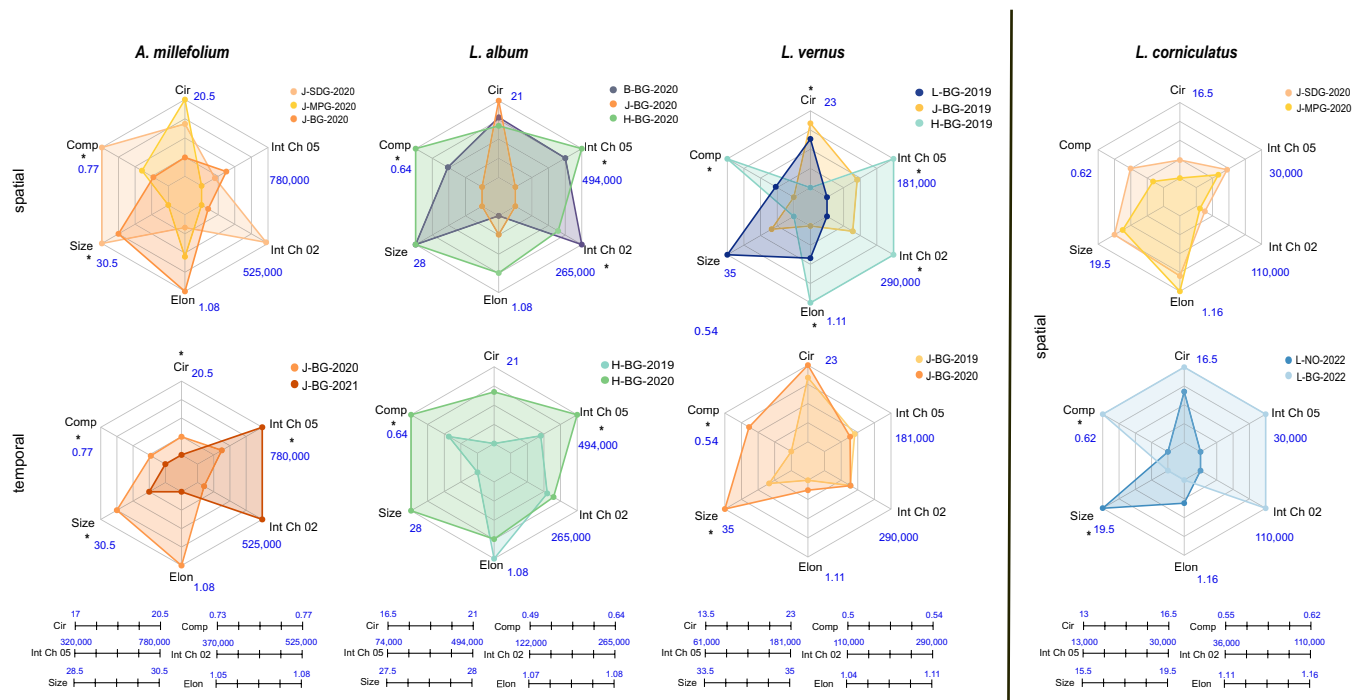


**FIGURE 2** | Spider charts for six selected pollen traits for four species studied (*Achillea millefolium*, *Lamium album*, *Lathyrus vernus*, and *Lotus corniculatus*), subdivided into spatial and temporal investigation. Only fully developed pollen were analyzed. For *L. corniculatus*, only spatial examination was possible, marked by the black vertical line. The selected traits are circularity, compactness, size, elongatedness, intensity Ch02 (green fluorescence intensity), and intensity Ch05 (red fluorescence intensity). Spatially, the sites were examined. Temporally, the time of collection was investigated in different years. Asterisks indicate a  $p$  value below 0.05. The scaling of the axes for each species was based on the minimum and maximum measured value for each spatial and temporal trait, marked by these corresponding number lines under the spider plots (Table 1). B-Berlin, BG—botanical garden, H-Halle, J-Jena, MPG—mesophilic grasslands, NO—urban open space, SDG—semi-natural dry grasslands. [Color figure can be viewed at [wileyonlinelibrary.com](https://onlinelibrary.wiley.com)]

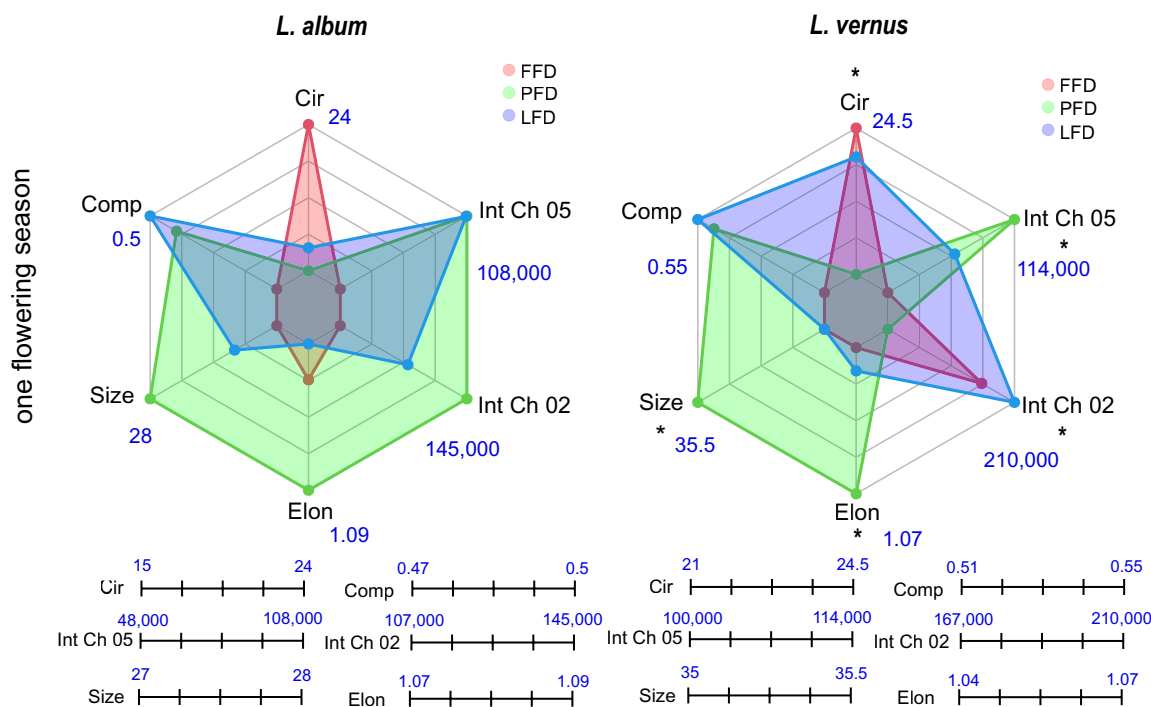


**FIGURE 3** | Spider charts for six selected pollen traits for two species studied (*Lamium album*, and *Lathyrus vernus*), for one flowering season. All samples (fully developed pollen only) were collected in the Botanical Garden in Jena in 2020. The selected traits are circularity (Cir), compactness (Comp), size (Size), elongatedness (Elon), intensity Ch02 (green fluorescence intensity) (Int Ch 02), and intensity Ch05 (red fluorescence intensity) (Int Ch 05). Asterisks indicate a  $p$ -value below 0.05. The scaling of the axes for each species was based on the minimum and maximum measured value for each trait, marked by these corresponding number lines under the spider plots (Table 1). FFD—first flowering day, LFD—last flowering day, PFD—peak flowering day. [Color figure can be viewed at [wileyonlinelibrary.com](https://onlinelibrary.wiley.com)]

beginning of the season (modal value:  $27\mu\text{m}$ ), largest at the end of the season (modal value:  $34\mu\text{m}$ ) and an intermediate size at the peak flowering day (modal value:  $27.5\mu\text{m}$ ). *L. album* and *L. vernus* have different ratios of undeveloped to developed pollen. The proportion of developed pollen was always clearly higher than the proportion of undeveloped pollen (Table S7). Compared to *L. album*, *L. vernus* has a higher proportion of undeveloped pollen in the total population than in the individual phenological phases.

### 3.3 | Machine Learning

The machine learning experiment revealed model accuracies for different combinations of datasets containing data for all four species but with one, two, or three different measurements included in the training dataset varying in sampling location or sampling year (Figure 5). Training with different random seeds for model initialisation revealed that accuracies vary less than 1%, allowing for qualitative assessments. Adding more measurements to the best training combination (backward) leads to stagnation of the identification accuracy. The addition of further better measurements (forward) leads to a significant improvement in identification accuracy for *L. album* and *L. vernus*. But also, for *A. millefolium* and *L. corniculatus*, the addition of further measurements led to a slight increase in identification accuracy. The best identification results were always obtained with at least three measurements,

regardless of whether these were the three best or the three worst measurements.

## 4 | Discussion

### 4.1 | Inter- and Intra-Specific Variation of Fully Developed Pollen

#### 4.1.1 | Pollen Size

In accordance with Hornick et al. [65] who recently demonstrated the good agreement of MIFC pollen size assessment for wind-pollinated plant pollen with classical literature [21], we also found comparable results for the four selected insect-pollinated species. In Beug [21], only 50 pollen grains per species were microscopically measured, mainly collected in the botanical garden Göttingen from 1997 to 2002. These samples were stored dry, measured after 2–4 years and treated with different chemicals (such as acetic and sulfuric acid). In contrast, average values per sample in our study were derived from 79 to 1249 (average 667) pollen grains per sample originating from different geographical origins and time points. Overall, the cytometrically measured size ranges agree with the described literature values for all species [21] ( $R^2=0.93$ ,  $y=0.8212x+2.935$ ). However, measured average size values were 9.8%–11.5% smaller than the mean literature values (Table 1). The slightly smaller size values in our study might

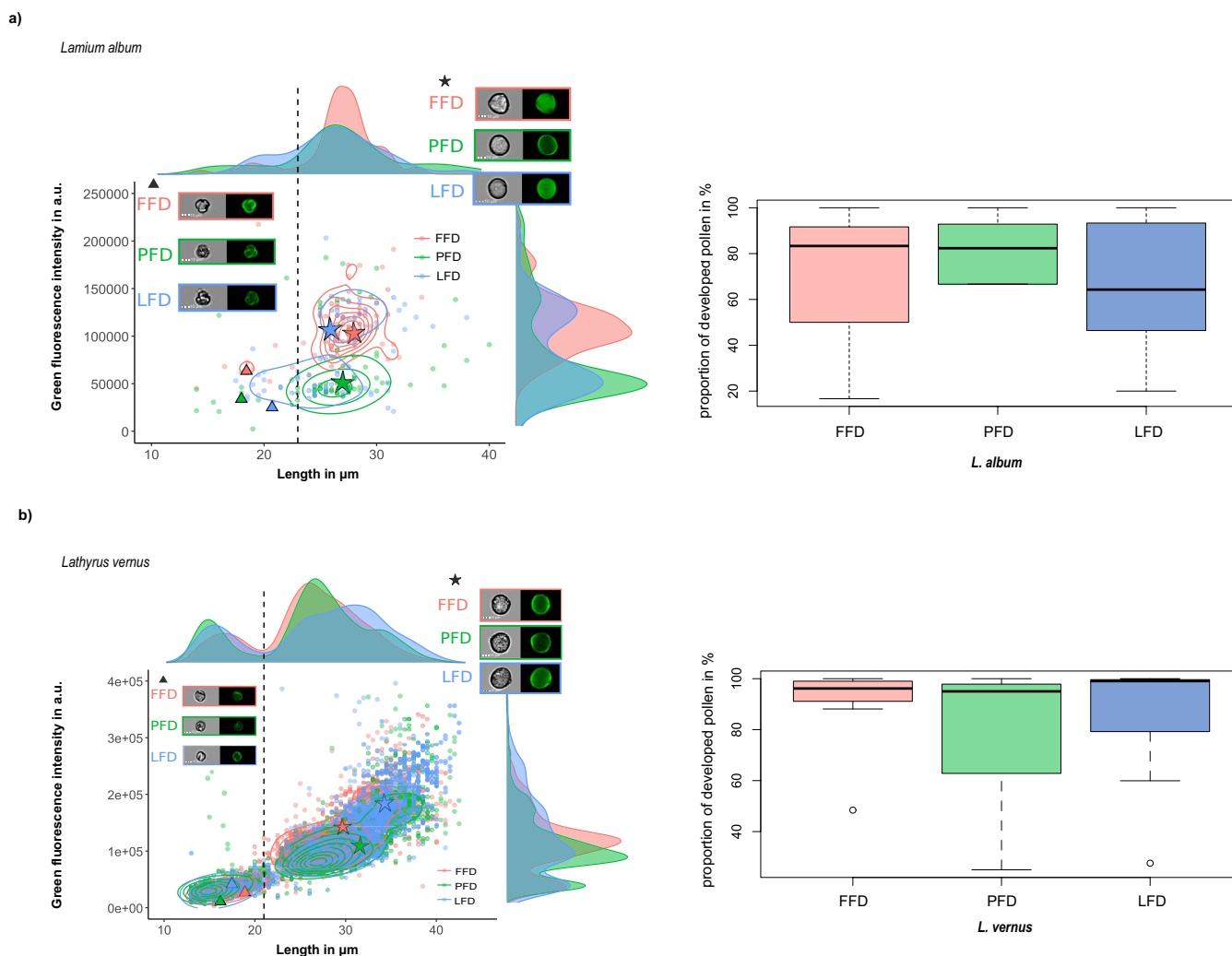


**FIGURE 4** | Density and dot plots for two selected traits for two studied species (a) *L. album*, (b) *L. vernus* on the left and boxplots with the percentage of developed pollen for the phenology stage on the right. The selected traits are pollen size and intensity Ch02 (green fluorescence intensity). Shown are the distributions at different sampling days during phenological development (first flowering day (FFD)—red, Peak flowering day (PFD)—green, last flowering day (LFD)—blue) and species. The dashed line indicates the threshold value that separates the populations. Microscopic images of developed pollen taken with MIFC for each of the three collection days are presented in the bright-field and green fluorescence channels, indicated by a star on the plot. Similarly, microscopic images of undeveloped pollen from the same collection days are shown for both channels and marked with a triangle on the plot. A paired *t*-test revealed no significant differences between the phenological stages, neither for *L. album* nor for *L. vernus*. [Color figure can be viewed at [wileyonlinelibrary.com](https://onlinelibrary.wiley.com)]

be related to different sample treatment as acetolytic pre-treatment can cause swelling of pollen grains [60].

Geographical origin might contribute to intraspecific variation in pollen size, possibly linked to variation in chromosome levels (ploidy) [49, 81]. Different ploidy levels could thus lead to altered pollen sizes in different geographical areas within Germany [82]. Warwick and Black [83] reported pollen sizes of 21.4–26.4  $\mu\text{m}$  for *A. millefolium* depending on the level of ploidy. In our study, the pollen size of *A. millefolium* varied in the range of 28.0–32.0  $\mu\text{m}$ , which could be related to differences in ploidy levels as described by Warwick and Black [83] and Storme et al. [52]. Ramsey [84] also showed for *Achillea millefolium* var. *borealis* (Bong.) ploidy-related size differences (2n—mean: 27.5  $\mu\text{m}$ ; n—mean: 19.0  $\mu\text{m}$ ). It should be noted that in this study, all possible viewing perspectives of the pollen were included in the analysis. This approach

may explain the high variation in pollen size observed in *L. corniculatus*, as its elliptic shape presents two distinct viewing angles: a polar view (round) and an equatorial view (elliptic).

#### 4.1.2 | Multivariate Trait Spaces

According to Hypothesis 1, we were able to demonstrate that intraspecific pollen trait variation was comparable to interspecific variation for fully developed pollen of all four species studied (Table 1). While the data of this study did not originate from a full-factorial designed experiment, we observed that certain pairwise combinations, comparing the same sampling locations but collected in different years or vice versa, revealed varying trait responses among species. These significant differences were specific to each species and varied in direction.

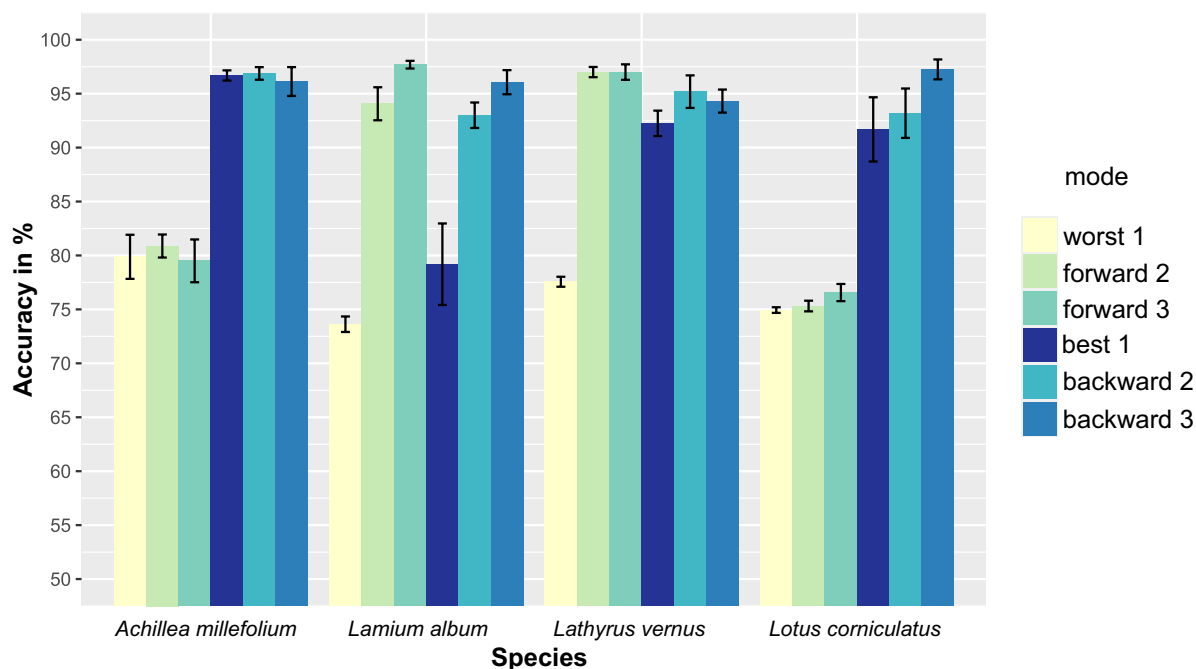


**FIGURE 5** | Bar chart for the averaged identification accuracy of the different combinations tested for each species. The colors correspond to the following combinations: worst 1 (forward 1)—light yellow, forward 2—light olive green, forward 3—light green, best 1 (backward 1)—dark blue, backward 2—turquoise, forward 3—light green and backward 3—dark turquoise. The numbers correspond to the different numbers (1–3) of measurements included in the training (see Table S8). [Color figure can be viewed at [wileyonlinelibrary.com](https://onlinelibrary.wiley.com/doi/10.1002/cyto.a.24932)]

Nevertheless, despite huge variations in sampling time and location, pollen of the species *A. millefolium* and the much smaller *L. corniculatus* were well distinguishable from the others based on morphology and fluorescence properties. On the other hand, *L. album* and *L. vernus* were shown to have more similar morphology and fluorescence properties, less well distinguishable, and were thus more prone to misclassifications.

One would expect pollen of *L. vernus* and *L. corniculatus*, both belonging to the same family Fabaceae, to be more similar in their pollen traits than *L. vernus* and *L. album* (Lamiaceae). But other studies have shown that similar pollen traits can also be related to similar pollinators. Schemske [85] found that two bee-pollinated tropical herbs, *Costus allenii* (Maas) and *Costus laevis* (Ruiz & Pav.), share the same pollinator and have converged in floral traits. Similarly, Basso-Alves et al. [86] observed that species within the same genus (in this case: *Erythrina*, *Macroptilium*, and *Mucuna*) with different pollinators have distinct pollen and stigma morphology as well.

#### 4.1.3 | Ecological Relevance of Investigated Pollen Traits

MIFC not only allows us to identify pollen in a sample, but the specific trait values could also help to understand plant-pollinator interactions better. Pollen size relates cubically to volume, thus potentially influencing the effectiveness of pollen sampling of pollinators. As a theoretical consideration, a 4 μm difference in size (as found in *L. corniculatus* pollen collected at two sites in Leipzig in two different years) would result in a doubling of pollen basket volume. Assuming a honey bee collects approximately 2,800 pollen grains in one

pollen flight (based on [87]), which would have an average size of 15.5 μm (site L-BG), the volume of the pollen basket would be ~5,459,486 μm<sup>3</sup>. But if the same collected pollen grains had a size of 19.5 μm (site L-NO), the volume would be ~10,870,775 μm<sup>3</sup>. This doubling of the volume would mean that pollinators would be more effective in pollen foraging when collecting the same number of pollen grains. This detailed information on spatio-temporal variations of pollen traits could be a relevant input parameter to models for insect behavior and foraging such as BEEHAVE [88].

One example of different species-specific responses to temporal and spatial variation is *L. corniculatus* pollen, which did not show any differences in pollen traits for the samples collected in the same time period in mesophilic and semi-dry grassland, whereas *A. millefolium* showed clear differences in pollen traits between the different habitats. We would have expected greater fluorescence intensity for all samples in the SDG samples, as these sites in Jena are located on southern-faced slopes, which are exposed to higher light intensities and would require higher DNA protection, potentially achieved by higher content of photoprotective pigments, resulting in higher fluorescence [89]. Wavelengths in the red fluorescence range are especially significant for pollen due to the presence of particular pigments and structural compounds, primarily sporopollenin and carotenoids. Sporopollenin, a resilient biopolymer in the outer pollen layer, confers robust protection against environmental stresses, including UV radiation, due to its chemical stability and resistance to degradation [90–92]. Carotenoids, meanwhile, absorb light in the blue and green spectra, reflecting and transmitting yellow-to-red light, thus producing the yellow-orange hue seen in many pollen types [93, 94]. One explanation for our non-significant results could be that differences in habitat types were not large enough, and one might only expect

differences along stronger gradients, such as in altitude. These aspects should be investigated in the future more systematically and for a broader range of species.

Overall, the fluorescence properties of pollen, especially insect-pollinated pollen, are still quite unexplored, but may be important for pollinator–plant interaction and pollinator attraction [95–97]. This fluorescence is thought to assist pollinators in more effectively recognizing pollen, potentially increasing pollination efficiency [96, 98].

## 4.2 | Phenological Pollen Trait Variation

The timing of flowering plays a crucial role in pollination success. For example, Kudo [99] found that later flowering can be advantageous for effective pollination for *Rhododendron aurum* (Georgi). Gallagher and Campbell [100] showed that manipulating the start of the flowering period leads to changes in pollination effectiveness. Additionally, it has been shown that changes in flowering times due to climate change can lead to changes in pollinator effectiveness [101].

The relationship between flowering time and pollen traits is also described as complex and dependent on many factors [100, 102–104]. Therefore, no study has yet been able to show a correlation between flowering periods and pollen traits. Interestingly, *A. millefolium* (June–October) and *L. corniculatus* (May–August) bloomed at different times and were also quite different in their morphology, while *L. vernus* and *L. album* both flower in April and May [105] and also showed similar morphological pollen traits. These results could provide an indication of a possible correlation between flowering time, as well as temporally related differences/similarities in pollinator species and pollen traits, but this would need to be investigated in more detail with more data.

According to Hypothesis 2, pollen trait variation during one flowering season was observed for both investigated species, and we observed bimodal pollen size distributions representing the undeveloped and developed pollen (Figure 3 and Figure 4). As expected, *L. album* and *L. vernus* pollen grains were rounder at the beginning of the flowering season (pollen swell before release, resulting in an increase of pollen volume due to material passing from the sporophyte and starch storage) compared to the remaining season, where they are expected to dehydrate during presentation [57, 106, 107] and thus become less circular. However, it is striking that only one of the two species (*L. album*  $p=0.609$ , *L. vernus*  $p=0.005$ ) showed a significant difference in pollen size within one flowering season (Figure 3). It is conceivable that the collection period of 23–69 days was too short to sample the pollen in sufficient quantities in all stages of the season. It is also possible that the small number of samples of *L. album* ( $n=86$ ) does not allow detection of more general results. Surprisingly, despite their different pollen sizes, *L. album* and *L. vernus* have a similar threshold ( $\sim 22\ \mu\text{m}$ ) separating the undeveloped and developed pollen. Contrary to our expectations, the proportion of developed pollen was always higher than the proportion of undeveloped pollen in the two species and the respective phenological stages. Here, too, the low number of samples and sampling days, especially for *L. album*, may be decisive.

The fluorescence properties of pollen change during development based on the decrease of oxygen and hydrogen and the increase of carbon [62, 108, 109]. For example, the undeveloped pollen of *Tussilago farfara* L. showed green fluorescence, while fully developed pollen showed mainly yellow fluorescence [62]. In our study, we could show that green fluorescence intensity was highest for *L. album* and *L. vernus* pollen during the maximum peak of flowering. The difference in highest green fluorescence in our study (PFD) compared to Roshchina [62] (FFD) might be explained by species-specific differences and an earlier flowering of *Tussilago farfara*, which also relates to different pollinator attraction. Urbanczyk et al. [109] studied spectral fluorescence variation of some *Ericaceae* taxa pollen and found that most of them had two fluorescing pollen populations (different sizes and fluorescence intensities). We also found two fluorescing pollen populations in our study, which could indicate different degrees of maturity of the pollen grains.

### 4.2.1 | Relevance for Automated Pollen Identification

As stated earlier, knowledge of potential pollen trait variation is relevant when creating a reference database for automated pollen recognition. Ideally, the training dataset should encounter a similar range of expected trait variation for the classification use cases.

According to our dataset, *A. millefolium* and *L. corniculatus* are easiest to discriminate by automated methods due to their large size differences. Even spatio-temporal intraspecific variation did not affect interspecific discrimination. Dunker et al. [28] already showed that *A. millefolium* could be determined with an accuracy of 98.7% (misclassification only with *Achillea distans* (Waldst. & Kit.)) and *L. corniculatus* with an accuracy of 100%.

In contrast, *L. album* and *L. vernus* revealed high similarity in the six pollen traits which were investigated, meaning that an automated classification of these two species is a more challenging task. Depending on year-to-year and site variation in their traits, the discrimination of these two species could be easier or more difficult. Notably, Olsson et al. [20] showed that misclassifications have also occurred in their data set for *L. album*.

A classical taxonomist would, for example, consider the pollen classes to discriminate the species (*Lamium*=Tricolpatae, *Lathyrus*=Tricolporatae). Therefore, in addition to the image features, it could be beneficial for such cases to consider image-based classification instead of relying only on derived feature values, which miss some spatial information, for example, about thickness of fluorescing exine, intine, or aperture type and location.

Fluorescence properties of the pollen are also suitable for pollen recognition and classification [28, 110–112]. With a success rate of 92%–97%, Ronneberger et al. [113] were able to classify 26 taxa using a combination of confocal microscopy and fluorescence pollen images.

A machine learning model should be applicable to complex processes in the real world. Therefore, robust automated pollen identification always requires that training data best encompass

the expected variation in the prediction dataset. It will thus be crucial when creating reference databases to consider relevant circumstances which affect trait variation in our case and keep them as comparable as possible (e.g., sample storage conditions, flowering time point). From stochastic learning theory, we know that the generalization error is bound by the information added to the classifier [114]. This is a logistical law where the rate at which the error is decreased slows down, and the amount of data needed to proceed grows exponentially because the new information added by each sample decreases when more samples are already known to the model. However, collecting and labeling data is expensive, so creating models is expensive. We observed that the samples collected at a specific time and location shared more commonalities than samples from different time points and locations. Therefore, it is very important to increase the number of different locations and times to increase the variation in data distribution to create a model that better represents the real world. Furthermore, the conducted machine learning experiment showed that multiple measurements have a positive effect on the robustness of identification accuracy. Consequently, we recommend collecting smaller numbers of samples over several years and collection sites rather than many samples in a few years and across few collection sites. However, we found indicators such as the comparison between best and worst accuracies based on pairwise sample comparisons that help guess when the model reaches its goal of modeling the intended process correctly. These observations are limited due to the size of the dataset, which is restricted to few locations, times, and species. Furthermore, we observed that the used subsampling method for balancing the data could significantly influence the results. Therefore, we recommend collecting data equally distributed over all combinations of species, locations, and times to tackle this caveat.

Despite all optimization attempts to discriminate between species using automated methods, it is important to note that for some taxa, traditional microscopic analysis of pollen can only be used to differentiate at the genus or family level. Traditional and new methods should be compared extensively, and in case that microscopic identification cannot be done at the species or genus level, a combination with other molecular techniques is recommended to verify the results.

## 5 | Conclusions and Outlook

The study shows that pollen traits can be more variable in temporal and spatial aspects than expected from pollen classification textbooks, showing species-specific trends. Since intraspecific variation in pollen traits could be demonstrated, this should also be taken into account when creating reference databases for automated pollen identification tools.

In the future, a more systematic understanding of causal relationships is needed, especially for pollen trait variation and traits which are not well studied such as pollen fluorescence and its interaction with pollinators. Our intention with this study was to provide a descriptive dataset to assess the potential variation which can be expected from different sites, years, and phenological stages. This builds the basis for future full-factorial experiments and power analysis coupled with

measures of ploidy, physical environments, and/or pollinator visitation.

### Author Contributions

F.W. collected, prepared, and measured samples, analyzed the data, and prepared the main draft together with T.H. and S.D., C.P., T.J.D., and A.L. collected and prepared samples. C.R., D.R., and W.S.H. contributed critical feedback during the writing process. M.H. performed the ML classifications. All authors contributed critically to the drafts and gave final approval for publication.

### Acknowledgments

The authors also thank all persons who helped with collecting data, curation of data: Nahid Paenroudoshti (sampling and annotation), Lea Reinke (annotation), Marcel Herrmann (annotation), Konstantin Albrecht (pollen extraction, measurements, annotation), all Botanical Gardens in Berlin, Halle, Jena, and Leipzig, especially Janin Naumann for the support in pollen collection and preparation.

### Conflicts of Interest

The patent submission EP000003692357A1/US020200278300A1 by S.D. could create a potential conflicts of interest, but to date no financial benefit has been accrued from the patent submission. A cooperation contract between UFZ and Cytek (Amsterdam, Netherlands) exists, regulating beta testing of products.

### Data Availability Statement

The data will be stored in the <https://zenodo.org/records/14858091> and in the FlowRepository: <http://flowrepository.org/experiments/7840>.

### References

1. R. Fattorini and B. J. Glover, "Molecular Mechanisms of Pollination Biology," *Annual Review of Plant Biology* 71 (2020): 487–515, <https://doi.org/10.1146/annurev-arplant-081519-040003>.
2. T. Doyle, W. L. S. Hawkes, R. Massy, G. D. Powney, M. H. M. Menz, and K. R. Wotton, "Pollination by Hoverflies in the Anthropocene," *Proceedings. Biological Sciences* 287, no. 1927 (2020): 20200508, <https://doi.org/10.1098/rspb.2020.0508>.
3. K. Dymond, J. L. Celis-Diez, S. G. Potts, B. G. Howlett, B. K. Willcox, and M. P. D. Garratt, "The Role of Insect Pollinators in Avocado Production: A Global Review," *Journal of Applied Entomology = Zeitschrift Fur Angewandte Entomologie* 145, no. 5 (2021): 369–383, <https://doi.org/10.1111/jen.12869>.
4. J. W. Millard, R. Freeman, and T. Newbold, "Text-Analysis Reveals Taxonomic and Geographic Disparities in Animal Pollination Literature," *Ecography* 43, no. 1 (2020): 44–59, <https://doi.org/10.1111/ecog.04532>.
5. J. Ollerton, R. Winfree, and S. Tarrant, "How Many Flowering Plants Are Pollinated by Animals?," *Oikos* 120, no. 3 (2011): 321–326, <https://doi.org/10.1111/j.1600-0706.2010.18644.x>.
6. A. Pardo and P. A. V. Borges, "Worldwide Importance of Insect Pollination in Apple Orchards: A Review," *Agriculture, Ecosystems & Environment* 293 (2020): 106839, <https://doi.org/10.1016/j.agee.2020.106839>.
7. J. P. Van der Sluijs and N. S. Vaage, "Pollinators and Global Food Security: The Need for Holistic Global Stewardship," *Food Ethics* 1, no. 1 (2016): 75–91, <https://doi.org/10.1007/s41055-016-0003-z>.
8. K. L. Bell, J. Fowler, K. S. Burgess, et al., "Applying Pollen DNA Metabarcoding to the Study of Plant–Pollinator Interactions,"

- Applications in Plant Sciences* 5, no. 6 (2017): apps.1600124, <https://doi.org/10.3732/apps.1600124>.
9. J. Bosch, A. M. M. González, A. Rodrigo, and D. Navarro, "Plant–Pollinator Networks: Adding the Pollinator's Perspective," *Ecology Letters* 12, no. 5 (2009): 409–419, <https://doi.org/10.1111/j.1461-0248.2009.01296.x>.
10. D. L. Byers and S.-M. Chang, "Studying Plant–Pollinator Interactions Facing Climate Change and Changing Environments," *Applications in Plant Sciences* 5, no. 6 (2017): apps.1700052, <https://doi.org/10.3732/apps.1700052>.
11. A. Gous, D. Z. H. Swanevelder, C. D. Eardley, and S. Willows-Munro, "Plant–Pollinator Interactions Over Time: Pollen Metabarcoding From Bees in a Historic Collection," *Evolutionary Applications* 12, no. 2 (2019): 187–197, <https://doi.org/10.1111/eva.12707>.
12. G. D. Jones, "Pollen Analyses for Pollination Research, Unacetolyzed Pollen," *Journal of Pollination Ecology* 9 (2012): 96–107, [https://doi.org/10.26786/1920-7603\(2012\)15](https://doi.org/10.26786/1920-7603(2012)15).
13. N. de Manincor, N. Hautekèete, C. Mazoyer, et al., "How Biased Is Our Perception of Plant–Pollinator Networks? A Comparison of Visit- and Pollen-Based Representations of the Same Networks," *Acta Oecologica* 105 (2020): 103551, <https://doi.org/10.1016/j.actao.2020.103551>.
14. G. Ballantyne, K. C. R. Baldock, and P. G. Willmer, "Constructing More Informative Plant–Pollinator Networks: Visitation and Pollen Deposition Networks in a Heathland Plant Community," *Proceedings. Biological Sciences* 282, no. 1814 (2015): 20151130, <https://doi.org/10.1098/rspb.2015.1130>.
15. N. E. Duffus, C. R. Christie, and J. Morimoto, "Insect Cultural Services: How Insects Have Changed Our Lives and How Can we Do Better for Them," *Insects* 12, no. 5 (2021): 377, <https://doi.org/10.3390/insects12050377>.
16. T. Hornick, A. Richter, W. S. Harpole, et al., "An Integrative Environmental Pollen Diversity Assessment and Its Importance for the Sustainable Development Goals," *Plants, People, Planet* 4, no. 2 (2022): 110–121, <https://doi.org/10.1002/ppp3.10234>.
17. K. L. Bell, N. De Vere, A. Keller, et al., "Pollen DNA Barcoding: Current Applications and Future Prospects," *Genome* 59, no. 9 (2016): 629–640, <https://doi.org/10.1139/gen-2015-0200>.
18. J. Buters, B. Clot, C. Galán, et al., "Automatic Detection of Airborne Pollen: An Overview," *Aerobiologia* 40, no. 1 (2024): 13–37, <https://doi.org/10.1007/s10453-022-09750-x>.
19. J. V. Marcos, R. Nava, G. Cristóbal, et al., "Automated Pollen Identification Using Microscopic Imaging and Texture Analysis," *Micron* 68 (2015): 36–46, <https://doi.org/10.1016/j.micron.2014.09.002>.
20. O. Olsson, M. Karlsson, A. S. Persson, et al., "Efficient, Automated and Robust Pollen Analysis Using Deep Learning," *Methods in Ecology and Evolution* 12, no. 5 (2021): 850–862, <https://doi.org/10.1111/2041-210X.13575>.
21. H.-J. Beug, *Leitfaden der Pollenbestimmung für Mitteleuropa und angrenzende Gebiete*, 2nd ed. (Verlag Dr. Friedrich Pfeil, 2015).
22. P. Carrión, E. Cernadas, J. F. Gálvez, M. Damián, and P. De Sá-Otero, "Classification of Honeybee Pollen Using a Multiscale Texture Filtering Scheme," *Machine Vision and Applications* 15, no. 4 (2004): 186–193, <https://doi.org/10.1007/s00138-004-0150-9>.
23. M. Rodríguez-Damian, E. Cernadas, A. Formella, M. Fernandez-Delgado, and P. De Sa-Otero, "Automatic Detection and Classification of Grains of Pollen Based on Shape and Texture," *IEEE Transactions on Systems, Man, and Cybernetics, Part C (Applications and Reviews)* 36, no. 4 (2006): 531–542, <https://doi.org/10.1109/TSMCC.2005.855426>.
24. N. Tsiknakis, E. Savvidaki, G. C. Manikis, et al., "Pollen Grain Classification Based on Ensemble Transfer Learning on the Cretan Pollen Dataset," *Plants (Basel, Switzerland)* 11, no. 7 (2022): 919, <https://doi.org/10.3390/plants11070919>.
25. K. Faegri and J. Iversen, *Bestimmungsschlüssel für die nordwesteuropäische Pollenflora* (G. Fischer, 1993).
26. P. D. Moore, J. A. Webb, and M. E. Collinson, *Pollen Analysis*, 2nd ed. (Blackwell Science Ltd., 1999).
27. K. von der Ohe and W. von der Ohe, "Celler Melissopalynologische Sammlung CMS," 2003.
28. S. Dunker, E. Motivans, D. Rakosy, et al., "Pollen Analysis Using Multispectral Imaging Flow Cytometry and Deep Learning," *New Phytologist* 229, no. 1 (2021): 593–606, <https://doi.org/10.1111/nph.16882>.
29. E. García-Forteza, A. García-Pérez, E. Gimeno-Páez, et al., "A Deep Learning-Based System (Microscan) for the Identification of Pollen Development Stages and Its Application to Obtaining Doubled Haploid Lines in Eggplant," *Biology* 9, no. 9 (2020): 272, <https://doi.org/10.3390/biology9090272>.
30. B. Crouzy, M. Stella, T. Konzelmann, B. Calpini, and B. Clot, "All-Optical Automatic Pollen Identification: Towards an Operational System," *Atmospheric Environment* 140 (2016): 202–212, <https://doi.org/10.1016/j.atmosenv.2016.05.062>.
31. K. A. Holt and K. D. Bennett, "Principles and Methods for Automated Palynology," *New Phytologist* 203, no. 3 (2014): 735–742, <https://doi.org/10.1111/nph.12848>.
32. G. D. Jones and V. M. Bryant, "A Comparison of Pollen Counts: Light Versus Scanning Electron Microscopy," *Grana* 46, no. 1 (2007): 20–33, <https://doi.org/10.1080/00173130601173897>.
33. Y. Kaya, M. E. Erez, O. Karabacak, L. Kayci, and M. Fidan, "An Automatic Identification Method for the Comparison of Plant and Honey Pollen Based on GLCM Texture Features and Artificial Neural Network," *Grana* 52, no. 1 (2013): 71–77, <https://doi.org/10.1080/00173134.2012.754050>.
34. K. Kraaijeveld, L. A. de Weger, M. Ventayol García, et al., "Efficient and Sensitive Identification and Quantification of Airborne Pollen Using Next-Generation DNA Sequencing," *Molecular Ecology Resources* 15, no. 1 (2015): 8–16, <https://doi.org/10.1111/1755-0998.12288>.
35. P. Viertel and M. König, "Pattern Recognition Methodologies for Pollen Grain Image Classification: A Survey," *Machine Vision and Applications* 33, no. 1 (2022): 18, <https://doi.org/10.1007/s00138-021-01271-w>.
36. A. Adadi, "A Survey on Data-Efficient Algorithms in Big Data Era," *Journal of Big Data* 8, no. 1 (2021): 24, <https://doi.org/10.1186/s40537-021-00419-9>.
37. C. Beleites, U. Neugebauer, T. Bocklitz, C. Krafft, and J. Popp, "Sample Size Planning for Classification Models," *Analytica Chimica Acta* 760 (2013): 25–33, <https://doi.org/10.1016/j.aca.2012.11.007>.
38. R. Geirhos, J.-H. Jacobsen, C. Michaelis, et al., "Shortcut Learning in Deep Neural Networks," *Nature Machine Intelligence* 2, no. 11 (2020): 665–673, <https://doi.org/10.1038/s42256-020-00257-z>.
39. M. Wang and W. Deng, "Deep Visual Domain Adaptation: A Survey," *Neurocomputing* 312 (2018): 135–153, <https://doi.org/10.1016/J.NEUCOM.2018.05.083>.
40. A. H. Wortley, H. Wang, L. Lu, D.-Z. Li, and S. Blackmore, "Evolution of Angiosperm Pollen," *Annals of the Missouri Botanical Garden* 100, no. 3 (2015): 177–226, <https://doi.org/10.3417/2012047>.
41. D. E. Rosen, R. T. Schuh, and G. L. Stebbins, "Flowering Plants: Evolution Above the Species Level," *Systematic Zoology* 24, no. 4 (1975): 504, <https://doi.org/10.2307/2412917>.
42. C. Torres, "Pollen Size Evolution: Correlation Between Pollen Volume and Pistil Length in Asteraceae," *Sexual Plant Reproduction* 12, no. 6 (2000): 365–370, <https://doi.org/10.1007/s004970000030>.

43. F. R. Ganders, "The Biology of Heterostyly," *New Zealand Journal of Botany* 17, no. 4 (1979): 607–635, <https://doi.org/10.1080/0028825X.1979.10432574>.
44. T. J. Deilmann, J. Ulrich, and C. Römermann, "Habitat Conditions Filter Stronger for Functional Traits Than for Phenology in Herbaceous Species," *Ecology and Evolution* 14, no. 6 (2024): e11505, <https://doi.org/10.1002/ece3.11505>.
45. C. Plos, N. Stelbrink, C. Römermann, T. M. Knight, and I. Hensen, "Abiotic Conditions Affect Nectar Properties and Flower Visitation in Four Herbaceous Plant Species," *Flora* 303 (2023): 152279, <https://doi.org/10.1016/j.flora.2023.152279>.
46. T. Altmann, B. Damm, W. B. Frommer, et al., "Easy Determination of Ploidy Level in *Arabidopsis thaliana* Plants by Means of Pollen Size Measurement," *Plant Cell Reports* 13, no. 11 (1994): 652–656, <https://doi.org/10.1007/BF00232939>.
47. T. Fukuhara, "Variation of Pollen and Ovule Parameters Among Different Ploidy Levels of *Corydalis* (Fumariaceae)," *Plant Systematics and Evolution* 224, no. 1–2 (2000): 1–12, <https://doi.org/10.1007/BF00985263>.
48. B. Johansen and R. Von Bothmer, "Pollen Size in *Hordeum* L.: Correlation Between Size, Ploidy Level, and Breeding System," *Sexual Plant Reproduction* 7, no. 5 (1994): 259–263, <https://doi.org/10.1007/BF00227707>.
49. A. Katsiotis and R. A. Forsberg, "Pollen Grain Size in Four Ploidy Levels of Genus *Avena*," *Euphytica* 83, no. 2 (1995): 103–108, <https://doi.org/10.1007/BF01678036>.
50. H. Sanders, "Polyploidy and Pollen Grain Size: Is There a Correlation?," 2021, <https://www.semanticscholar.org/paper/Polyploidy-and-Pollen-Grain-Size%3A-Is-There-a-Sanders/7c2e110fe05e42d42572c0d80b1046d05cd723a9>.
51. S. Srisuwan, D. Sihachakr, J. Martín, et al., "Change in Nuclear DNA Content and Pollen Size With Polyploidisation in the Sweet Potato (*Ipomoea batatas*, Convolvulaceae) Complex," *Plant Biology* 21, no. 2 (2019): 237–247, <https://doi.org/10.1111/plb.12945>.
52. N. de Storme, L. Zamariola, M. Mau, T. F. Sharbel, and D. Geelen, "Volume-Based Pollen Size Analysis: An Advanced Method to Assess Somatic and Gametophytic Ploidy in Flowering Plants," *Plant Reproduction* 26, no. 2 (2013): 65–81, <https://doi.org/10.1007/s00497-012-0209-0>.
53. C. R. Bell, "Mineral Nutrition and Flower to Flower Pollen Size Variation," *American Journal of Botany* 46, no. 9 (1959): 621–624, <https://doi.org/10.1002/j.1537-2197.1959.tb07062.x>.
54. E. Pers-Kamczyc, Ż. Tyrała-Wierucka, M. Rabska, D. Wrońska-Pilarek, and J. Kamczyc, "The Higher Availability of Nutrients Increases the Production but Decreases the Quality of Pollen Grains in *Juniperus communis* L.," *Journal of Plant Physiology* 248 (2020): 153–156, <https://doi.org/10.1016/j.jplph.2020.153156>.
55. H. J. Young and M. L. Stanton, "Influence of Environmental Quality on Pollen Competitive Ability in Wild Radish," *Science (New York, N.Y.)* 248, no. 4963 (1990): 1631–1633, <https://doi.org/10.1126/science.248.4963.1631>.
56. H. Fatmi, S. Mâalem, B. Harsa, A. Dekak, and H. Chenchouni, "Pollen Morphological Variability Correlates With a Large-Scale Gradient of Aridity," *Web Ecology* 20, no. 1 (2020): 19–32, <https://doi.org/10.5194/we-20-19-2020>.
57. G. Frenguelli, F. Ferranti, E. Tedeschini, and R. Andreutti, "Volume Changes in the Pollen Grain of *Corylus avellana* L. (Corylaceae) During Development," *Grana* 36, no. 5 (1997): 289–292, <https://doi.org/10.1080/00173139709362619>.
58. D. Kremer, E. Stabentheiner, and Ž. Borzan, "Pollen Traits of Some American Ashes Investigated by a Scanning Electron Microscope," 2005, <https://www.semanticscholar.org/paper/Pollen-traits-of-some-Ameri-can-ashes-investigated-a-Kremer-Stabentheiner/7e2c8f6c18a29b1ddf1a2105cd7dd404845cc35e>.
59. R. Kriebel, M. Khabbazian, and K. J. Sytsma, "A Continuous Morphological Approach to Study the Evolution of Pollen in a Phylogenetic Context: An Example With the Order Myrtales," *PLoS One* 12, no. 12 (2017): e0187228, <https://doi.org/10.1371/journal.pone.0187228>.
60. E. M. Mäkelä, "Size Distinctions Between *Betula* Pollen Types—A Review," *Grana* 35, no. 4 (1996): 248–256, <https://doi.org/10.1080/00173139609430011>.
61. C. Pöhlker, J. A. Huffman, J.-D. Förster, and U. Pöschl, "Autofluorescence of Atmospheric Bioaerosols: Spectral Fingerprints and Taxonomic Trends of Pollen," *Atmospheric Measurement Techniques* 6, no. 12 (2013): 3369–3392, <https://doi.org/10.5194/amt-6-3369-2013>.
62. V. V. Roshchina, "Autofluorescence of Plant Secreting Cells as a Biosensor and Bioindicator Reaction," *Journal of Fluorescence* 13, no. 5 (2003): 403–420, <https://doi.org/10.1023/A:1026164922760>.
63. J. Brooks and G. Shaw, "Chemical Structure of the Exine of Pollen Walls and a New Function for Carotenoids in Nature," *Nature* 219, no. 5153 (1968): 532–533, <https://doi.org/10.1038/219532a0>.
64. B. Nordt, I. Hensen, S. F. Bucher, et al., "The PhenObs Initiative: A Standardised Protocol for Monitoring Phenological Responses to Climate Change Using Herbaceous Plant Species in Botanical Gardens," *Functional Ecology* 35, no. 4 (2021): 821–834, <https://doi.org/10.1111/1365-2435.13747>.
65. T. Hornick, "High-Throughput Assessment of Anemophilous Pollen Size and Variability Using Imaging Cytometry," *New Phytologist* (2025), <https://doi.org/10.1111/nph.70070>.
66. R Core Team, *R: A Language and Environment for Statistical Computing* (R Foundation for Statistical Computing, 2022), <https://www.R-project.org/>.
67. H. Wickham, *ggplot2. Elegant Graphics for Data Analysis* (Springer International Publishing, 2016).
68. J. Oksanen, G. Simpson, F. Blanchet, et al., "Vegan: Community Ecology Package," 2022.
69. M. Nakazawa, *Fmsb: Functions for Medical Statistics Book With Some Demographic Data* (R package version 0.7.6, 2024), <https://cran.r-project.org/web/packages/fmsb>.
70. D. Kahle and H. Wickham, "ggmap: Spatial Visualization With ggplot2," 2013.
71. M. P. Arbizu, "pairwiseAdonis: Pairwise Multilevel Comparison Using Adonis," 2017.
72. I. Heidmann and M. Di Berardino, "Impedance Flow Cytometry as a Tool to Analyze Microspore and Pollen Quality," *Methods in Molecular Biology (Clifton, N.J.)* 1669 (2017): 339–354, [https://doi.org/10.1007/978-1-4939-7286-9\\_25](https://doi.org/10.1007/978-1-4939-7286-9_25).
73. Z. Zhong, L. Zheng, G. Kang, S. Li, and Y. Yang, "Random Erasing Data Augmentation," *Proceedings of the AAAI Conference on Artificial Intelligence* 34, no. 7 (2020): 13001–13008, <https://doi.org/10.1609/aaai.v34i07.7000>.
74. H. Zhang, M. Cisse, Y. N. Dauphin, and D. Lopez-Paz, "mixup: Beyond Empirical Risk Minimization," 2017, <http://arxiv.org/pdf/1710.09412.pdf>.
75. S. Yun, D. Han, S. J. Oh, S. Chun, J. Choe, and Y. Yoo, "CutMix: Regularization Strategy to Train Strong Classifiers With Localizable Features," 2019, <http://arxiv.org/pdf/1905.04899.pdf>.
76. E. D. Cubuk, B. Zoph, J. Shlens, and Q. Le, V, "RandAugment: Practical Automated Data Augmentation With a Reduced Search Space," 2019, <http://arxiv.org/pdf/1909.13719.pdf>.

77. D. P. Kingma and J. Ba, "Adam: A Method for Stochastic Optimization," 2014, <http://arxiv.org/pdf/1412.6980.pdf>.
78. I. Loshchilov and F. Hutter, "SGDR: Stochastic Gradient Descent With Warm Restarts," 2016, <http://arxiv.org/pdf/1608.03983.pdf>.
79. K. He, X. Zhang, S. Ren, and J. Sun, "Deep Residual Learning for Image Recognition," 2015, <http://arxiv.org/pdf/1512.03385>.
80. S. Liu, L. Qi, H. Qin, J. Shi, and J. Jia, "Path Aggregation Network for Instance Segmentation," 2018, <http://arxiv.org/pdf/1803.01534.pdf>.
81. R. Zhao, L. Xu, X. Xu, Y. Li, S. Xiao, and D. Yuan, "Comparative Study on Pollen Viability of *Camellia Oleifera* at Four Ploidy Levels," *Agronomy* 12, no. 11 (2022): 2592, <https://doi.org/10.3390/agronomy12112592>.
82. D. Wrońska-Pilarek, A. M. Jagodziński, J. Bocianowski, M. Marecik, and M. Janysek-Sołtysiak, "Pollen Morphology and Variability of *Sambucus nigra* L.—Adoxaceae," *Biologia* 75, no. 4 (2020): 481–493, <https://doi.org/10.2478/s11756-019-00396-8>.
83. S. I. Warwick and L. Black, "The Biology of Canadian Weeds: 52. *Achillea millefolium* L. S.L.," *Canadian Journal of Plant Science* 62, no. 1 (1982): 163–182, <https://doi.org/10.4141/CJPS82-024>.
84. J. Ramsey, "Unreduced Gametes and Neopolyploids in Natural Populations of *Achillea borealis* (Asteraceae)," *Heredity* 98, no. 3 (2007): 143–150, <https://doi.org/10.1038/sj.hdy.6800912>.
85. D. W. Schemske, "Floral Convergence and Pollinator Sharing in Two Bee-Pollinated Tropical Herbs," *Ecology* 62, no. 4 (1981): 946–954, <https://doi.org/10.2307/1936993>.
86. J. P. Basso-Alves, K. Agostini, and S. d. P. Teixeira, "Pollen and Stigma Morphology of Some Phaseoleae Species (Leguminosae) With Different Pollinators," *Plant Biology* 13, no. 4 (2011): 602–610, <https://doi.org/10.1111/j.1438-8677.2010.00416.x>.
87. D. A. Kendall and M. E. Solomon, "Quantities of Pollen on the Bodies of Insects Visiting Apple Blossom," *Journal of Applied Ecology* 10, no. 2 (1973): 627, <https://doi.org/10.2307/2402306>.
88. M. A. Becher, V. Grimm, P. Thorbek, J. Horn, P. J. Kennedy, and J. L. Osborne, "BEEHAVE: A Systems Model of Honeybee Colony Dynamics and Foraging to Explore Multifactorial Causes of Colony Failure," *Journal of Applied Ecology* 51, no. 2 (2014): 470–482, <https://doi.org/10.1111/1365-2664.12222>.
89. J. Rozema, R. A. Broekman, P. Blokker, et al., "UV-B Absorbance and UV-B Absorbing Compounds (Para-Coumaric Acid) in Pollen and Sporopollenin: The Perspective to Track Historic UV-B Levels," *Journal of Photochemistry and Photobiology B: Biology* 62, no. 1–2 (2001): 108–117, [https://doi.org/10.1016/S1011-1344\(01\)00155-5](https://doi.org/10.1016/S1011-1344(01)00155-5).
90. E. Domínguez, J. A. Mercado, M. A. Quesada, and A. Heredia, "Pollen Sporopollenin: Degradation and Structural Elucidation," *Sexual Plant Reproduction* 12, no. 3 (1999): 171–178, <https://doi.org/10.1007/s004970050189>.
91. F.-S. Li, P. Phyto, J. Jacobowitz, M. Hong, and J.-K. Weng, "The Molecular Structure of Plant Sporopollenin," *Nature Plants* 5, no. 1 (2019): 41–46, <https://doi.org/10.1038/s41477-018-0330-7>.
92. R. J. Scott, "Pollen Exine—The Sporopollenin Enigma and the Physics of Pattern," in *Molecular and Cellular Aspects of Plant Reproduction*, ed. R. J. Scott and A. D. Stead (Cambridge University Press, 1994), 49–82.
93. H. Hashimoto, C. Uragami, and R. J. Cogdell, "Carotenoids and Photosynthesis," *Sub-Cellular Biochemistry* 79 (2016): 111–139, [https://doi.org/10.1007/978-3-319-39126-7\\_4](https://doi.org/10.1007/978-3-319-39126-7_4).
94. R. Mărgăoan and M. Cornea-Cipcigan, "Carotenoids and Vitamins of Pollen," in *Pollen Chemistry & Biotechnology*, ed. N. E. Bayram, A. Ž. Kostic, and Y. C. Gercek (Springer International Publishing, 2023), 147–177.
95. A. R. Golt and L. J. Wood, "Glyphosate-Based Herbicides Alter the Reproductive Morphology of *Rosa acicularis* (Prickly Rose)," *Frontiers in Plant Science* 12 (2021): 698202, <https://doi.org/10.3389/fpls.2021.698202>.
96. S. Mori, H. Fukui, M. Oishi, et al., "Biocommunication Between Plants and Pollinating Insects Through Fluorescence of Pollen and Anthers," *Journal of Chemical Ecology* 44, no. 6 (2018): 591–600, <https://doi.org/10.1007/s10886-018-0958-9>.
97. S. Mori, S. Shimma, H. Masuko-Suzuki, et al., "Fluorescence From Abnormally Sterile Pollen of the Japanese Apricot," *Plant Biotechnology* 38, no. 3 (2021): 355–366, <https://doi.org/10.5511/plantbiotechnology.21.0730a>.
98. R. G. Stanley and H. F. Linskens, "Pollen Pigments," in *Pollen. Biology, Biochemistry, Management*, ed. R. G. Stanley and H. F. Linskens (Springer, 1974), 223–246.
99. G. Kudo, "Relationships Between Flowering Time and Fruit Set of the Entomophilous Alpine Shrub, *Rhododendron Aureum* (Ericaceae), Inhabiting Snow Patches," *American Journal of Botany* 80, no. 11 (1993): 1300, <https://doi.org/10.2307/2445714>.
100. M. K. Gallagher and D. R. Campbell, "Pollinator Visitation Rate and Effectiveness Vary With Flowering Phenology," *American Journal of Botany* 107, no. 3 (2020): 445–455, <https://doi.org/10.1002/ajb2.1439>.
101. N. E. Rafferty and A. R. Ives, "Pollinator Effectiveness Varies With Experimental Shifts in Flowering Time," *Ecology* 93, no. 4 (2012): 803–814, <https://doi.org/10.1890/11-0967.1>.
102. J. Forrest and J. D. Thomson, "Consequences of Variation in Flowering Time Within and Among Individuals of *Mertensia fusiformis* (Boraginaceae), an Early Spring Wildflower," *American Journal of Botany* 97, no. 1 (2010): 38–48, <https://doi.org/10.3732/ajb.0900083>.
103. I. Kim, M. J. Kwak, J. K. Lee, et al., "Flowering Phenology and Characteristics of Pollen Aeroparticles of *Quercus* Species in Korea," *Forests* 11, no. 2 (2020): 232, <https://doi.org/10.3390/f11020232>.
104. G. Kudo and L. D. Harder, "Floral and Inflorescence Effects on Variation in Pollen Removal and Seed Production Among Six Legume Species," *Functional Ecology* 19, no. 2 (2005): 245–254, <https://doi.org/10.1111/j.1365-2435.2005.00961.x>.
105. T. Schauer, C. Caspari, and S. Caspari, *Die Pflanzen Mitteleuropas. Über 1500 Arten* (BLV Buchverl, 2012).
106. H. Halbritter, S. Ulrich, F. Grimsson, et al., *Illustrated Pollen Terminology*, 2nd ed. (Springer Nature, 2018).
107. E. Pacini, "From Anther and Pollen Ripening to Pollen Presentation," *Plant Systematics and Evolution* 222, no. 1/4 (2000): 19–43, <http://www.jstor.org/stable/23644326>.
108. J. C. Audran and M. T. M. Willemse, "Wall Development and Its Autofluorescence of Sterile and Fertile *Vicia faba* L. Pollen," *Protoplasma* 110, no. 2 (1982): 106–111, <https://doi.org/10.1007/BF01281536>.
109. J. Urbanczyk, M. A. Fernandez Casado, T. E. Díaz, P. Heras, M. Infante, and A. G. Borrego, "Spectral Fluorescence Variation of Pollen and Spores From Recent Peat-Forming Plants," *International Journal of Coal Geology* 131 (2014): 263–273, <https://doi.org/10.1016/j.coal.2014.06.024>.
110. P. Kron, A. Kwok, and B. C. Husband, "Flow Cytometric Analysis of Pollen Grains Collected From Individual Bees Provides Information About Pollen Load Composition and Foraging Behaviour," *Annals of Botany* 113, no. 1 (2014): 191–197, <https://doi.org/10.1093/aob/mct257>.
111. K. Mitsumoto, K. Yabusaki, and H. Aoyagi, "Classification of Pollen Species Using Autofluorescence Image Analysis," *Journal of Bioscience and Bioengineering* 107, no. 1 (2009): 90–94, <https://doi.org/10.1016/j.jbiosc.2008.10.001>.

112. R. K. Tennant, R. T. Jones, F. Brock, et al., "A New Flow Cytometry Method Enabling Rapid Purification of Fossil Pollen From Terrestrial Sediments for AMS Radiocarbon Dating," *Journal of Quaternary Science* 28, no. 3 (2013): 229–236, <https://doi.org/10.1002/jqs.2606>.
113. O. Ronneberger, E. Schultz, and H. Burkhardt, "Automated Pollen Recognition Using 3D Volume Images From Fluorescence Microscopy," *Aerobiologia* 18, no. 2 (2002): 107–115, <https://doi.org/10.1023/A:1020623724584>.
114. V. N. Vapnik, *The Nature of Statistical Learning Theory*, 2nd ed. (Springer, 2000).

### Supporting Information

Additional supporting information can be found online in the Supporting Information section.